Supporting Information

In Situ Luminescence Thermometry to Locally Measure Temperature Gradients during Catalytic Reactions

Robin G. Geitenbeek[1,‡], *Anne-Eva Nieuwelink*[2,‡], *Thimo S. Jacobs*[2], *Bastiaan B. V. Salzmann*[1], *Joris Goetze*[2], *Andries Meijerink*[1,*], *Bert M. Weckhuysen*[2,*]

1 Condensed Matter and Interfaces, 2 Inorganic Chemistry and Catalysis

Debye Institute for Nanomaterials Science, Utrecht University, Universiteitsweg 99, 3584 CG Utrecht, The Netherlands

*Corresponding authors: A.Meijerink@uu.nl, B.M.Weckhuysen@uu.nl

A. Experimental Section

Chemicals. All chemicals were used without further purification. The following chemicals were purchased from Sigma-Aldrich: Cyclohexane (99.5%, CH), oleic acid (90%, OA), ethanol (>99.8%, EtOH), methanol (>99.85%, MeOH), sodium fluoride (>98%, NaF), sodium hydroxide (>97%, NaOH), ammonium fluoride (>98%, NH_4F), ammonium hydroxide (28 wt% in H_2O, ammonia) lanthanide acetate hydrates (99.9%, $Ln(Ac)_3$), tetraethyl orthosilicate (99.999%,

TEOS) and IGEPAL CO-520 ($(C_2H_4O)_n$•$C_{15}H_{24}O$ with n ~ 5, average Mn = 441 g mol^{-1}, NP-5). 1-octadecene (90%, ODE) was purchased from Acros Organics. Yttrium fluoride (>99.99%, YF_3) was purchased from ChemPur. Ytterbium fluoride (>99.99%, YbF_3) was purchased from Strem Chemicals. Erbium fluoride (>99.99%, ErF_3) was purchased from Highways Internationals. Spherical α-Al_2O_3 (99.9% metals basis, average particle size 20-50 μm) was purchased from Alfa Aesar.

Preparation of microcrystalline $NaYF_4$. Microcrystalline $NaYF_4$ doped with 19% Yb^{3+} and 2% Er^{3+} ($NaYF_4$:Er,Yb), was prepared via a solid state synthesis[1]. In short, 15 mmol of dried NaF, 15 mmol of REF_3 (RE = Y, Er, Yb) and 13.5 mmol of NH_4F were mixed with a pestle and mortar and afterwards placed in an alumina crucible. The mixture was fired in the oven in an excess of NH_4F under a nitrogen atmosphere. The samples were heated to 573 K for 3 h and afterwards heated to 823 K for 8 h. The heating rate was 5 K min^{-1} for both heating steps. The obtained powder was pressed into pellets, crushed and sieved. Afterwards, temperature-dependent luminescence studies have been performed as shown in Figure S1a. The sieve fraction of 150-425 μm was used during the experiments.

Preparation of $NaYF_4$@SiO_2 NPs. $NaYF_4$@SiO_2 nanoparticles (NPs) doped with 19% Yb^{3+} and 2% Er^{3+} of ca. 50 nm were prepared via an initial synthesis of $NaYF_4$ core particles (ca. 20 nm) and subsequent SiO_2 overgrowth as reported earlier[2-5].

Deposition of $NaYF_4$@SiO_2 NPs on α-Al_2O_3 support. The $NaYF_4$@SiO_2 NPs were deposited on spherical α-Al_2O_3 by adding a known concentration of the NPs in EtOH to ca. 300 mg α-Al_2O_3 (sieve fraction >75 μm). This mixture was equilibrated for 1 min to allow for the NPs to adsorb on the alumina surface before filtering the $NaYF_4$@SiO_2/α-Al_2O_3. The product obtained

was washed with EtOH and dried overnight in static air at 333 K. Afterwards, temperature-dependent luminescence studies have been performed as shown in Figure S1b.

Preparation of $NaYF_4/SiO_2$ NPs in extrudates. The $NaYF_4/SiO_2$ NPs were prepared as described above and subsequently dried to obtain a powder. Afterwards, 3.2 g of powder was mixed with H_2O, 3.8 g silica (Davicat Si1302) and 0.2 g methylcellulose (4000 CP, Sigma Aldrich) in a Caleva Mixer Torque Rheometer. The obtained paste was then transferred to a single mini-screw extruder (Caleva) and extruded into 2 mm diameter cylindrical extrudates. The obtained extrudates were dried overnight at room temperature and afterwards calcined at 873 K. Afterwards, temperature-dependent luminescence studies have been performed as shown in Figure S1c.

Preparation of H-ZSM-5 catalyst. The catalyst for the Methanol-to-Hydrocarbons (MTH) reaction was a commercially available zeolite ZSM-5 from Zeolyst with a crystal size of 200-800 nm and Si/Al ratio of 25. In order to convert the zeolite into its H-form the zeolite powder was calcined at 823 K (5 K min^{-1}) for 10 h in air and afterwards pressed into pellets, crushed and sieved. The sieve fraction of 212-425 μm was used during the experiments.

In situ reactor setup. The MTH reaction was performed in a rectangular fixed bed quartz reactor (ID = 6 mm × 3 mm), filled with 165 mg catalyst and 165 mg temperature probes (T-probes). This leads to a volume ratio of ca. 5:1 catalyst/T-probes. Before the reaction, the reactor bed was activated at 823 K in 100% O_2 for 1 h. The reaction was performed with a total weight hourly space velocity (WHSV) of 15 h^{-1} in a He flow with 18% MeOH saturation. This was obtained by flowing He through a MeOH saturator, kept at 303 K. All reaction products were analyzed using an online Interscience Compact GC equipped with an Rtx-wax and Rtx-1 column

in series and an Rtx-1, Rt-TCEP and Al_2O_3/Na_2SO_4 in series, both connected to an FID. The total reactor bed was typically 21 mm high and an Avantes high-tempearture optical fiber probe was placed at three different heights along the bed as shown in Figure S2. The probe contained 6 excitation fibers and 1 detection fiber with diameters of 400 µm. The probe was placed several mm from the reactor bed to ensure no overlap between the different measurement spots and a sufficient signal acquisition. A 980 nm continuous wave laser (0.5 W) was used to excite the sample via the probe before subsequent collection of the upconversion emission via the same probe. The collected light was led to an AvaSpec-2048L spectrometer via a short pass filter to filter out the excitation light source. The temperature calibration measurements were performed by the same spectrometry setup in combination with a Linkam THMS600 Microscope Stage. SEM images were made using a Phenom ProX.

B. Figures

Luminescence characterization and calibration. Luminescence studies of all three different systems showed temperature-dependent luminescence behavior, as shown in Figure S1. Luminescence spectra were obtained upon excitation at 980 nm with intervals of 25 K from 300 K (black spectrum) up to 900 K (orange spectrum). The spectra are normalized on the maximum intensity of the peak centered at around 541 nm.

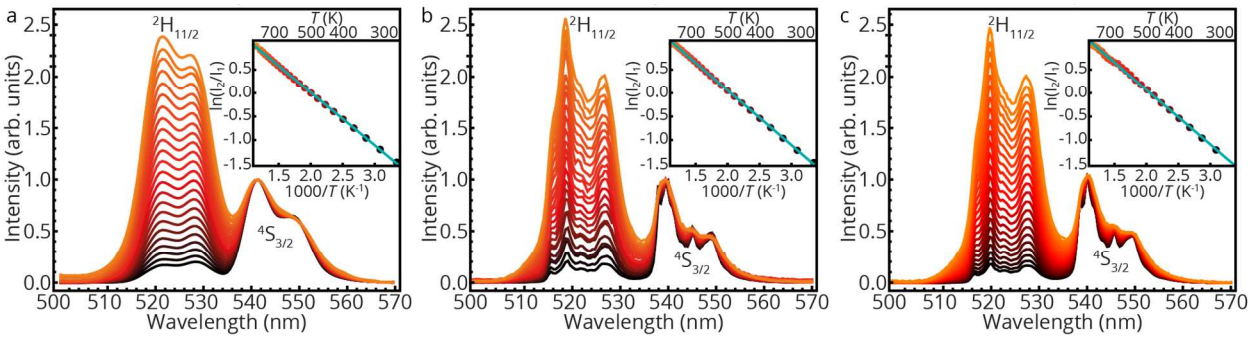

Figure S1. Temperature-dependent luminescence spectra of $NaYF_4$ microcrystals (a), $NaYF_4$ NPs on Al_2O_3 (b) and $NaYF_4$ NPs in extrudates (c) upon excitation at 980 nm. The emission spectra are normalized on the $^4S_{3/2}$-$^4I_{15/2}$ emission peak (540-550 nm). The inset shows the linear correlation between the logarithm of the ratio of the two emission peaks vs reciprocal temperature.

The emission peaks originate from the $^4S_{3/2}$-$^4I_{15/2}$ (at 541 nm) and $^2H_{11/2}$-$^4I_{15/2}$ (at 525 nm) interconfigurational f-f transitions of Er^{3+} after excitation of two Yb^{3+} ions and subsequent upconversion energy transfer[6].

Figure S1 clearly shows that the $^2H_{11/2}$-$^4I_{15/2}$ emission intensity increases with respect to the $^4S_{3/2}$-$^4I_{15/2}$ emission upon increasing temperatures (black to orange). This temperature-dependent luminescence derives from the small energy difference between the $^4S_{3/2}$ and $^2H_{11/2}$ states, which was determined to be ca. 700 cm^{-1} (several kT) from the spectra at 300 K. Due to the small energy difference between the $^2H_{11/2}$ and the $^4S_{3/2}$ state, thermal energy is sufficient to efficiently facilitate fast equilibration between the two excited states and therefore the two states are thermally coupled. Consequently, the populations of the two excited states is governed by a Boltzmann distribution,[7] as shown in equation S1.

$$\frac{N_2}{N_1} = \exp\left(\frac{-\Delta E}{kT}\right) \qquad \text{(S1)}$$

Here, N_2 and N_1 are the populations from state i, ΔE the energy difference between the two excited states, k the Boltzmann constant and T the temperature. Equation S1 shows that the ratio between N_2 and N_1 becomes higher with increasing temperature, which is in line with our observations in Figure S1. The emission intensity is proportional to the population and therefore we can rewrite equation S1, resulting in equation S2.

$$\ln\left(\frac{I_2}{I_1}\right) = \ln C - \frac{\Delta E}{kT} \qquad (2)$$

Here, the logarithm of the ratio of the emission intensities (I_2/I_1) scales linearly with reciprocal temperature as shown in the inset of Figure S1. The linear behavior could be fitted (blue lines) with linear fits and from the steepness of the curve the ΔE could be calculated. The calculated values of 700-750 cm^{-1} correspond well with the value of ca. 700 cm^{-1} obtained from the room temperature spectra.

Figure S1 shows that the temperature-dependent emission follows a clear trend, which can be exploited to determine unknown temperatures upon readout of the emission spectrum and subsequent calculation of the emission intensity ratio.

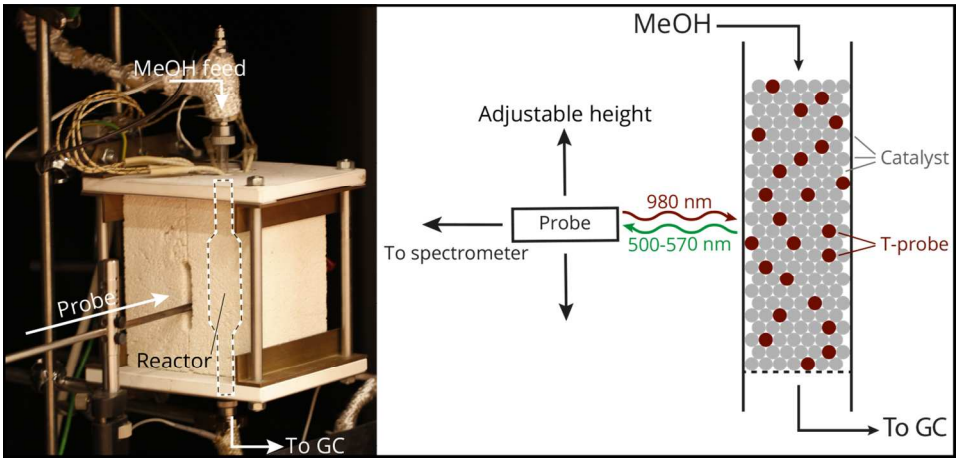

Figure S2. Photograph of the setup used during in situ temperature measurements and a schematic representation of the fixed bed quartz reactor filled with catalyst and $NaYF_4$:Er,Yb. The MeOH is introduced from the top and all reaction products were analyzed with an online GC. An optical fiber probe was placed at three different heights of the reactor bed. In order to

minimize the collection of specular reflection of the excitation laser, the reactor was axially rotated in such a way that the excitation laser hit the quartz window at an angle of ca. 120 degrees.

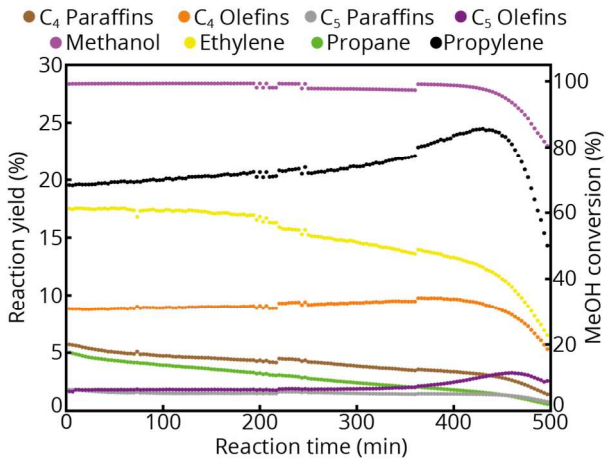

Figure S3. Products obtained during the reaction as determined by online GC. The products are plotted on the left y-axis, while the MeOH conversion was plotted on the right y-axis. The higher carbon species ($\geq C_6$ olefins and paraffins, aromatics and coke) are no longer distinguishable with the GC and therefore not shown here.

References

1. Aarts, L.; van der Ende, B. M.; Meijerink, A. Downconversion for Solar Cells in $NaYF_4$:Er,Yb *J. Appl. Phys.* **2009**, 106, 23522.
2. Geitenbeek, R.; Prins, P. T.; Albrecht, W.; van Blaaderen, A.; Weckhuysen, B. M.; Meijerink, A. $NaYF_4:Er^{3+},Yb^{3+}/SiO_2$ Core/Shell Upconverting Nanocrystals for Luminescence Thermometry up to 900 K *J. Phys. Chem. C* **2017**, 121, 3503-3510.
3. Koole, R.; van Schooneveld, M. M.; Hilhorst, J.; de Mello Donegá, C.; Hart, D. C. 't; van Blaaderen, A.; Vanmaekelbergh, D.; Meijerink, A. On the Incorporation Mechanism of Hydrophobic Quantum Dots in Silica Spheres by a Reverse Microemulsion Method *Chem. Mater.* **2008**, 20, 2503–2512.
4. Li, Z. & Zhang, Y. An Efficient and User-Friendly Method for the Synthesis of Hexagonal-Phase $NaYF_4$:Yb,Er/Tm Nanocrystals with Controllable Shape and Upconversion Fluorescence *Nanotechnology* **2008**, 19, 345606.
5. Wang, F., Deng, R. & Liu, X. Preparation of Core-Shell $NaGdF_4$ Nanoparticles Doped with Luminescent Lanthanide Ions to be used as Upconversion-Based Probes *Nat. Protoc.* **2014**, 9, 1634–1644
6. Menyuk, N.; Dwight, K.; Pierce, J. W. $NaYF_4$:Yb,Er - An Efficient Upconversion Phosphor *Appl. Phys. Lett.* **1972**, 21, 159–161.
7. Brites, C. D. S.; Lima, P. P.; Silva, N. J. O.; Millán, A.; Amaral, V. S.; Palacio, F.; Carlos, L. D. Thermometry at the Nanoscale *Nanoscale* **2012**, 4, 4799–4829.